Acta Oceanol. Sin., 2010, Vol.29, No.1, p.79-87
DOI: 10.1007/s13131-010-0010-6
http://www.hyxb.org.cn
E-mail: hyxbe@263.net

Spatial variations of tidal water level and their impact on the exposure patterns of tidal land on the central Jiangsu coast

WANG Zhenyan[1,2*], GAO Shu[3], HUANG Haijun[1]

[1] Key Laboratory of Marine Geology and Environment, Chinese Academy of Sciences, Qingdao 266071, China

[2] Graduate School, Chinese Academy of Sciences, Beijing 100039, China

[3] MOE Key Laboratory for Coast and Island Development, Nanjing University, Nanjing 210093, China

Received 11 December 2008; accepted 7 April 2009

Abstract
The exposed area of intertidal zone varies with tidal water level changes. If intercomparisons of satellite images are adopted as a method to determine geomorphological changes of the intertidal zone in response to accretion or erosion processes, then the effect of water level variations must be evaluated. In this study, two Landsat TM images overpassing the central Jiangsu coastal waters on 2 January and 7 March 2002, respectively, were treated by the changing detection analysis using Image Differencing and Post-classification Comparison. The simultaneous tide level data from four tide gauge stations along the coast were used for displaying the spatial variations of water levels and determining the elevations of waterlines. The results show that the spatial variations of water levels are highly significant in the central Jiangsu coastal waters. The huge differences of tidal land exposure patterns between the two imaging times are related mainly to the spatial variations of tidal water levels, which are controlled by the differences in tidal phases for different imaging times and the spatial variations of water level over the study area at each imaging time. Under complex tidal conditions, e.g., those of the central Jiangsu coastal waters, the tide-surge model should be used to eliminate effectively the effects of water level variations on remote sensing interpretation of geomorphological changes in the intertidal zone.

Key words: waterline, water level variations, exposure patterns, central Jiangsu coast, remote sensing

1 Introduction

The intertidal zone, which is located between the high and low water levels on tidally dominated coasts, represents an important interface for land-ocean interactions. Geomorphological changes (i.e., erosion and accretion) of this environment exert a large impact on the human activities in coast areas. The intertidal zone is often characterized by rapid changes in terms of both size and position, but such changes are difficult to monitor by means of in situ survey. Thus, the technique of remote sensing has an advantage to obtain instantaneous geomorphological information, and the imagery can be retrieved periodically to form a time series (Ryu et al., 2008; Zhao et al., 2008; Zheng et al., 2007; Chang et al., 2004; Han et al., 2003; Mason et al., 2001; Kevin and Hesham, 1999; Mason et al. 1999; Chen and Rau, 1998; Mason et al., 1995; Frihy et al., 1994; Huang et al., 1994). By analyzing the time series, the patterns of spatial and temporal changes in the intertidal area may be identified.

The extent of exposed tidal land is controlled by a number of factors, including the hypsometric relationship of the intertidal zone (i.e., the area as a function of bed elevation) and the phase of tidal water level changes. In order to determine accurately the geomorphological changes, the effect of water level changes must be eliminated. For this purpose, some researchers have adopted the method of shoreline comparison (Chang et al., 2004; Li et al., 2004; Kevin and Hesham, 1999; Frihy et al., 1994) or co-tidal waterline comparison (Han et al., 2003; Huang et al., 1994). The

Foundation item: The Ministry of Science and Technology of China under contract No. 2006CB708410; the National Natural Science Foundation of China (NSFC) under contract No. 40706027.
*Corresponding author, E-mail: zywang@ms.qdio.ac.cn

former requires accurate interpretation of the position of shorelines from the remote sensing images. For intertidal areas with extensive tidal flats, although it is difficult to determine accurately the position of high water [because the signal indicating this characteristic line is illegible and changeable (Boak and Turner, 2005)], the instantaneous waterline is relatively easy to identify (Ryu et al., 2002; Lee et al., 2001). The latter requires that the images are associated with the same tidal level. Co-tidal images might be selected from a number of remote sensing images obtained in the past, but the availability of suitable images and morphological evolution of the tidal land would be a serious problem. Because the instantaneous waterline on the remote sensing image is ubiquitous, some researchers have attempted to use a series of images taken within a short period of time to figure out the waterline representing the intertidal elevation mark. The waterline and tide gauge data may be combined to formulate the Digital Elevation Model (DEM) of the intertidal zone, for analyzing the geomorphological changes with time (Ryu et al., 2008; Zhao et al., 2008; Zheng et al., 2007; Mason et al., 2001; Mason et al., 1999; Chen and Rau, 1998; Mason et al., 1995). The premise to establish the intertidal DEM on the basis of waterline comparison is that the position of the waterline on the intertidal zone represents a fixed elevation. Such an approach implies that: (1) the temporal change of the hypsometric curve of the intertidal zone can be neglected for the period of time during which the images are collected; and (2) the waterline over the region in consideration represents the same elevation (Zhao et al., 2008; Lin, 1991). The first assumption is approximately valid if net erosion or accretion is insignificant during the time interval for the two images (Zhao et al., 2008; Chen and Rau, 1998; Mason et al., 1995). However, the variations of tidal water level and their effects on remote sensing interpretation have been rarely discussed. Thus, the purpose of the present study is to identify the variations of tidal water level in coastal waters, taking the central Jiangsu coast as an example, and analyze their effects on exposure patterns of the intertidal zone and remote sensing interpretations of tidal land geomorphological changes.

2 The study area

The study area is located off the central Jiangsu coastlines (Fig. 1), which consists of a typical tidal mudflat area and a sandbank field. The sandbanks in this region are mostly submerged by sea water during high water periods, but the intertidal parts of the sandbanks cover a large area. The sandbank system consists of more than 70 linear sandbanks, which take a radial shape. The sandbanks have a total area of around 22 470 km^2, with 3 782 km^2 being above the 0 m bathymetry in terms of Chart Datum (Wang, 2002; Ren, 1986).

According to the previous research work, the main composition of these sandbanks is fine sand and silt which are derived from the estuarine sediment of the paleo-Changjiang River, while clayey materials were derived from the paleo-Huanghe River which discharged into the northern Jiangsu area in late Holocene periods (Wang, 2002). The source of modern sediment for the intertidal areas is affected by three sedimentary processes, i.e., the disposal of suspended sediment from the Changjiang River Estuary in the south, the southward transport of sediment generated by coastal erosion over the abandoned Huanghe River delta, and the sedimentary materials from reworking of the offshore sandbank system by tidal currents. In response to these processes, the sandbank system tends to migrate southward and westward (Huang and Li, 1998).

The tides in this area are semi-diurnal in character, with a mean tide range of 2.5–4 m (Ren, 1986). As shown on the co-tidal chart of the southern Huanghai Sea (Fig. 1), the co-tidal and co-range lines around the radial sandbank area show some approximate semicircles shapes which indicate that the tidal waves from the northeastern, eastern and southeastern open-sea synchronously converge at this area with almost the same propagation velocity. With Jiangang being the center, the mean tide range progressively decreases towards the south or the north (Lin et al., 2000; Lee et al., 1998). The maximum tide range is usually found between Jianggang and Xiaoyanggang (Ren, 1986).

3 Materials and methods

3.1 *Remote sensing images and analytical method*

Two sets of TM images of the study area, imaged on 2 January 2002 and 7 March 2002 (both at 10:19 am, Beijing time), are used for interpreting intertidal waterline information (in the following text, they are expressed as Image 20020102 and Image 20020307, respectively). In addition to data processing procedures

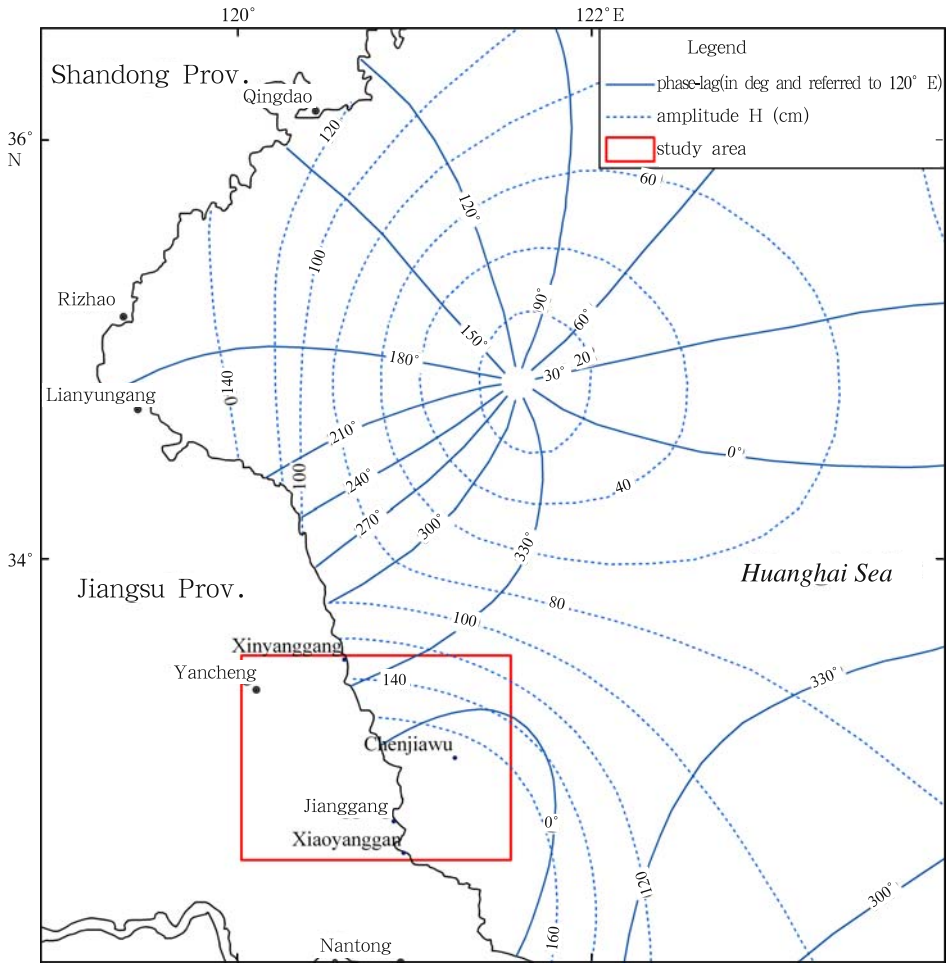

Fig.1. Location of the study area and the M_2 Co-tidal Chart for the southern Huanghai Sea [adapted from Lee et al. (1998)].

of geometric rectification, relative radiometric normalisation and the study area sub-setting, the two images are treated by change detection analysis using Image Differencing and Post-classification Comparison, respectively (Jensen, 2007). The Image Differencing subtracts the image parameters on Image 20020307 from Image 20020102 band by band and pixel by pixel. For Landsat TM images, the short-wave bands 5, 3 and 2 represent the infrared, red and green bands, respectively. According to the characteristics of spectral radiation and reflection, red and infrared bands are associated with strong reflection on land areas (including exposed tidal flats) but intense absorption in water areas, while the green band has the opposite characteristics (Jensen, 2007; Zhao, 2003). In order to distinguish between emerged intertidal flat and seawater, bands 5, 3 and 2 of the differenced image are selected for generating a pseudo-colour image. Post-classification comparison was undertaken using Geographic Information System (ArcGis), and spatial measurements and overlapping analysis were conducted for the waterline data, which were extracted from the above mentioned two images using unsupervised classification method (Dang et al., 2003). The transformed information obtained by Image Differencing alone may require further identification and classification for ground objects on the resultant image. Furthermore, the information obtained by post-classification comparison alone does not demonstrate the modified information in detail, which may cause misreading. However, the integrated application of both methods can increase the objectiveness and accuracy of information interpretation.

3.2 *Determination of tidal water level associated with the images*

Spatial variations in tidal water level over a coastal area can be determined using local tide gauge data. The results of the harmonic analysis of the

histori cal gauging data have been used for tide prediction (Fang et al., 1986). In China, tide tables are published each year by the National Marine Data and Information Service (NMDIS). The difference between the tidal data listed in the tide tables and those from measurements is influenced by a number of factors such as error in measurements and weather conditions (Xu, 1996). Generally, the accuracy of tide water level prediction for the major gauge stations is in the order of 20–30 cm (NMDIS, 2001).

In the present study, the predicted tide water level data of the Xinyanggang, Chenjiawu, Jianggang and Xiaoyanggang gauge stations are used to derive the tidal hydrographs at the various stations in the study area, by an interpolation algorithm, for the days in which the satellite images were obtained (i.e., 2 January 2002 and 7 March 2002). The interpolation algorithm is expressed as:

$$h = \frac{1}{2}(Z_0 + Z_1) + R\cos(\omega t), \tag{1}$$

where h is the height of tide, Z_0 and Z_1 are the elevations associated with high and low water times, respectively, R is the amplitude of water level variations, and ω is the angular rate of tidal water level variation.

4 Results and discussion

4.1 *Morphological stability of the study area*

The position of waterline on the exposed flat is controlled by the regional tidal action. Thus, if the morphology of the sandbanks is stable, then the extent of exposure shown on a remote sensing image reflects the tidal effect, i.e., the phase of water level change within a tidal cycle. In situ survey data have shown that the annual accretion/erosion rate is below 10 cm (6.6 cm on average) for the sand banks in the study area (Zhu and Fu, 1986). Because the gradient for the intertidal zone of the sandbanks is generally smaller than 1∶3 000, it can be deduced that the horizontal shift of a contour or bathymetric line in response to accretion/erosion should not exceed 300 m/a, i.e., the vertical accretion/erosion rate should not exceed 1.7 cm/a (6 cm/a maximum). Hence, in two months' time, the horizontal shift of the contour or bathymetric line should be within 50 m. Since the spatial resolution of the main bands of TM image (bands 1–5 and 7) is 30 m, the variation in the position of any bathymetric line over the study area during the two months should cover no more than two pixels on the image. This observation means that, on the temporal scale of two months, the sandbanks can be considered as being morphologically stable, so that any significant changes in the position of the waterline associated with a given tidal water level do not result from the sandbank morphology changes.

4.2 *Spatial variations in water level at different gauge stations*

The water level hydrographs for the Xinyanggang, Chenjiawu, Jianggang and Xiaoyanggang stations on 2 January and 7 March are plotted in Fig 2. From these data sets, the tidal range and water level data of each of the gauge stations, for the two satellite imaging days are obtained (Figs 3 and 4).

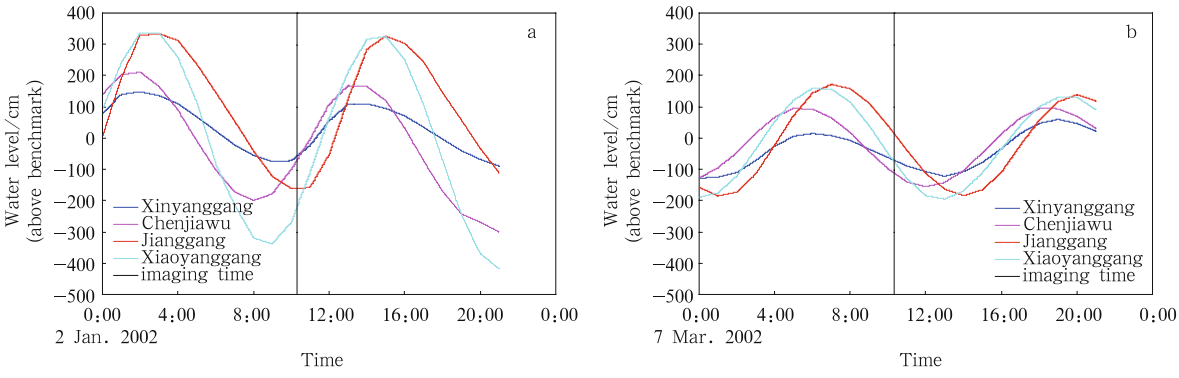

Fig.2. Water level hydrograph of Xinyanggang, Chenjiawu, Jianggang, and Xiaoyanggang gauging stations on 2 January 2002 (a) and 7 March 2002 (b).

The comparison of the hydrograph from the four tide gauge stations indicates that, on 2 January 2002 (spring tide), three of the stations, i.e., the Xinyanggang, Chenjiawu and Xiaoyanggang stations, were at an early stage during the flood phase of the tide when the satellite passed through this area, while the Jiang-

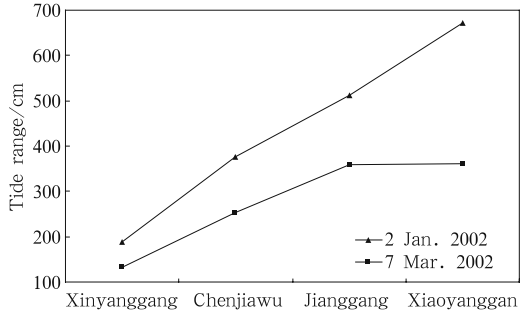

Fig.3. Tide range of Xinyanggang, Chenjiawu, Jianggang, and Xiaoyanggang gauging stations on 2 January 2002 and 7 March 2002.

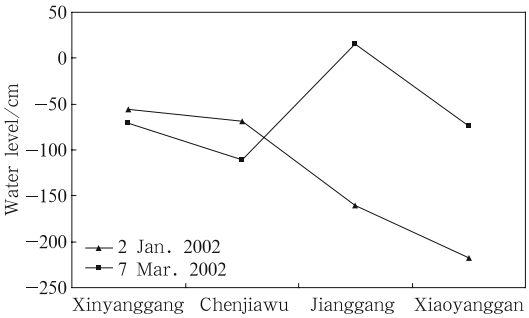

Fig.4. Water level of Xinyanggang, Chenjiawu, Jianggang, and Xiaoyanggang gauging stations at satellite imaging time on 2 January 2002 and 7 March 2002.

gang station was still in the low water slack (Fig. 2a). The tidal range during that day increased from the north towards the south, with notable differences (Fig. 3). On 7 March 2002 (neap tide), the four stations were all in the ebb phase of the tide when the satellite was passing though the study area (Fig. 2b). There is also an increase in tidal range from the north towards the south, with smaller difference than that during the spring tide (Fig. 3). Comparisons of the water level data of the four stations show that the water level in the north (represented by the Xinyanggang and Chenjiawu stations) was 110–150 cm higher than that in the south (represented by the Jianggang and Xiaoyanggang stations) at the satellite imaging time on 2 January 2002. The water level pattern was different for the day of 7 March 2002: in the north of the study area, the water level was generally lower than that in the south by 0–120 cm, and the difference in water level over the northern part was smaller than that of the southern part (Fig. 4). It is found that the water levels for the area between Chenjiawu and Jianggang at the two imaging times were nearly the same. Thus, there was a significant difference in the spatial variation patterns for water level between the two satellite imaging times.

4.3 *Detected changes in intertidal zone exposure patterns*

The composed pseudo-color image by image differencing for the two TM images (bands 5, 3 and 2) is shown in Fig. 5. On this image, the color of tidal flat

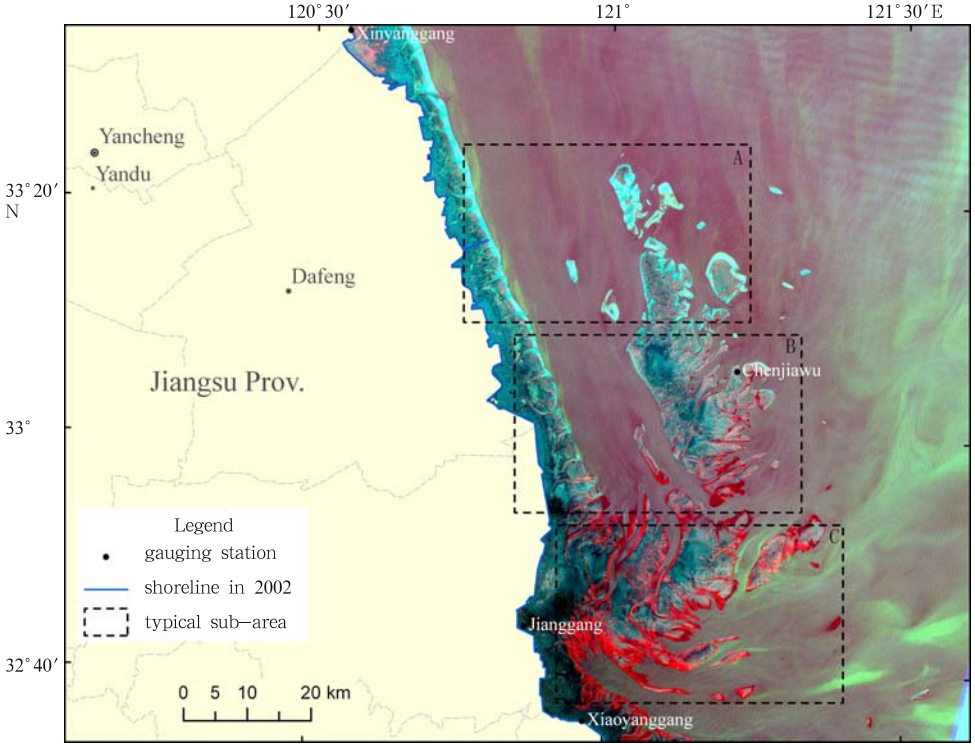

Fig.5. Composed pseudo-color image resulting from image differencing analysis.

close to waterline is significantly different from that of the inundated areas. The color of tidal flat edge is light blue in the north while that it is red in the south. This phenomenon reflects an "apparent" change in the tidal flat morphology. According to the characteristics of spectral radiation and reflection, the light blue area in Fig. 5 represents an "apparent increase" in the exposed intertidal area during 2 January to 7 March 2002. Likewise, the red edge in the south represents an "apparent decrease" in the exposed area. In order to identify the difference in the exposure patterns for different locations, we selected three sub-areas (A, B, and C) with the same size (1 269 km^2) for further analysis (Fig. 5).

The waterlines on the two images were extracted by using unsupervised classification method, and the exposed tidal flat areas at the two imaging times were obtained (Table 1). The exposed tidal flat areas in the two images are compared by using ArcGis spatial analysis and area measurements (Fig. 6; Table 1). On such a basis, the variations of the exposure area for the three sub-areas are derived and listed in Table 2.

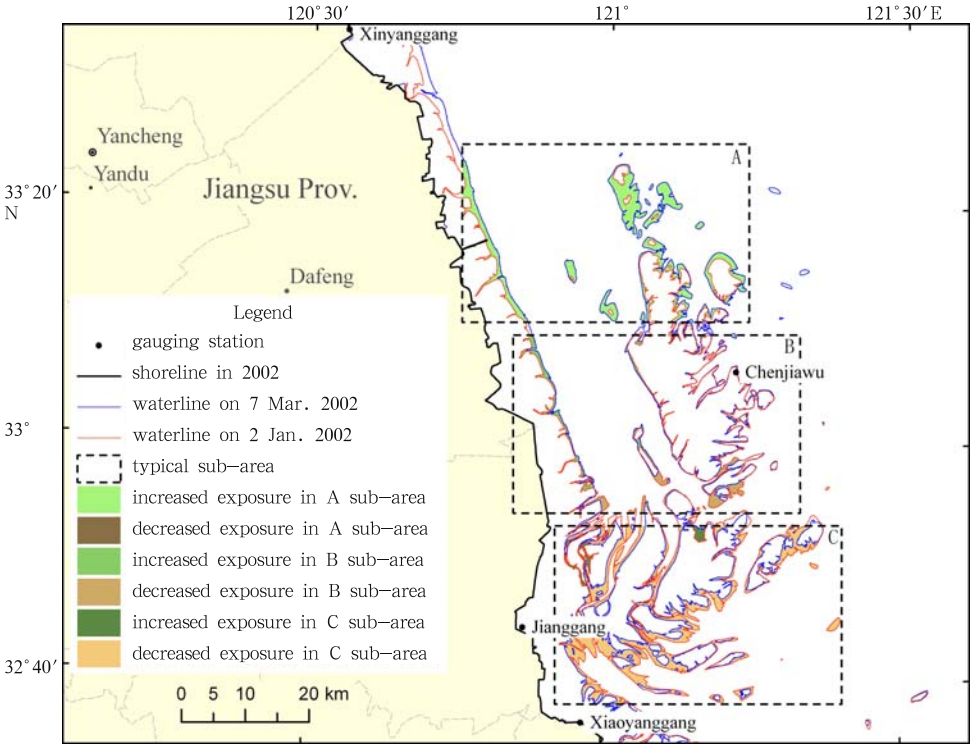

Fig.6. Result of post-classification comparison between images of 2 January 2002 and 7 March 2002.

Table 1. Comparison of classification results between Image 20020102 and Image 20020307

Exposure patterns	Pieces	Total area/km^2	Average area/km^2
Exposed areas on Image 20020102	47	1 677.746	35.697
Exposed areas on Image 20020307	106	1 632.060	15.397
Deceased exposed areas on Image 20020307	35	250.434	7.155
Increased exposed areas on Image 20020307	69	204.747	2.967
Total exposure variation	–	–45.686	–

Figure 5 indicates that the overall exposed area on Image 20020307 is larger than that on Image 20020102, but the exposure of the south part on the former image is smaller than that on the latter. Such an exposure pattern is consistent with the variations in water level of the study area (Fig. 4).

There were 106 pieces of exposed areas (including those huge pieces of tidal flats along the shoreline) on Image 20020307, whilst there were only 47 pieces on Image 20020102. The average exposure area on Image 20020307 was 1 632.060 km^2 in total (15.397 km^2 on average), whilst it was 1 677.746 km^2 in total (35.697 km^2 on average) for Image 20020102. Compared with the water levels of the four gauge stations at the two

Table 2. Variation of the exposed areas in the three sub-areas between Image 20020102 and Image 20020307

Exposure pattern	Sub-area	Pieces	Total area/km^2	Average area/km^2
Decreased exposure	A	100	0.474	0.005
	B	600	35.616	0.059
	C	150	177.993	1.187
Increased exposure	A	146	113.804	0.779
	B	648	31.846	0.049
	C	132	13.285	0.101
Net increase of exposed areas	A	–	113.330	–
	B	–	–3.770	–
	C	–	–164.708	–

imaging times, this phenomenon can be related to the fact that the water level on 7 March was generally higher than that on 2 January, reducing the total exposure and generating an increased number of pieces of exposed areas. The exposure in the middle and the southern parts of the study area on Image 20020102 was much larger than that on Image 20020307, but the situation in the north was just the opposite. For the exposed pieces shown on the 2 January image, 35 pieces were smaller in size than that on Image 20020307, with a total of 250.434 km^2 reduction; on the other hand, for the exposed pieces shown on Image 20020307, there were 69 enlarged pieces (in comparison with Image 20020102), with a total expanded area of only 204.747 km^2.

For the three typical sub-areas, the sub-area A has a larger exposed area on Image 20020307 than that on Image 20020102, B has an insignificant difference, and C has a smaller exposed area on Image 20020307. Furthermore, the three sub-areas have both increased and decreased parts, on the basis of a comparison between the two images. The reduced exposure on Image 20020307, as outlined above, is associated mainly with the sub-area C, with a reduced area of 177.993 km^2; the reduced area in the sub-area B is 35.616 km^2 and it is only 0.474 km^2 in A. Likewise, the increased exposure on Image 20020307 for sub-area A is 113.804 km^2, much larger than those of B (31.846 km^2) and C (13.285 km^2). As a result, the spatial change in the exposure pattern has an opposite trend: the magnitude of decrease is larger in the south than that in the north, but the magnitude of increase is larger in the north than that in the south. The net variation of the exposed areas for sub-area B is the smallest (3.770 km^2), as compared with 164.708 km^2 for C and 113.330 km^2 for A, indicating that sub-area B is located at a transitional position. Such net variations of sub-areas A, B and C are consistent with the observation that the water level in the middle and southern parts on Image 20020307 was higher than that on Image 20020102, but in the north the water level was lower on Image 20020307 than that on Image 20020102.

4.4 *Effect of water level variation on exposure pattern interpretation*

As analyzed above, the study area is morphologically stable during the interval of the two satellite imaging times. The exposed tidal flat areas of the two images show a contrary change trend in the northern and southern parts of the study area because the water level in the north-south direction changed in opposite direction. These results show that the waterline over the coastal zone with converging-diverging tidal conditions do not always mean a same elevation level. Therefore, the results of changes in the exposure pattern derived from comparison of images for different times may not represent real morphological changes (i.e., changes due to accretion or erosion). In order to identify the morphological changes using co-tidal waterline comparison, or to construct an intertidal DEM by the waterline method, it is important to fix the water level over the entire study area at the imaging time. In addition, the gradient of tidal flats is usually small, a slight vertical change in water level will cause a large horizontal migration of waterline on the tidal flat. Therefore, when the waterlines are used as strict elevation marks the effect of water level fluctuation caused by meteorological factors (such as wind wave) at the satellite imaging time must also be evaluated.

5 Conclusions

The example from the Jiangsu coast indicates that water level variations between different coastal sites may exist widely. The huge differences of tide-

land exposure patterns between the two imaging times on 2 January and 7 March 2002 are mainly caused by the variations of tidal water levels. The spatial variations of water levels in the central Jiangsu coastal waters are highly significant and can seriously affect the remote sensing interpretation of geomorphological changes in the intertidal zone. In a large coastal region, the water level variations are controlled by the differences in tidal phase and the instantaneous spatial variations of water level over the study area; therefore, the water level conditions observed at a single gauge station may fail to represent the overall conditions. Hence, a sufficient number of gauge stations are required to obtain representative conditions so that water level correction for different images can be carried out and realistic intertidal DEMs can be formulated. For coastal areas with straight shoreline and simple tidal dynamics, the water level may be determined by linear interpolation using data collected from neighboring gauge stations (Yun, 2005; Zhang and Xiao, 1995). However, for any coastal areas with tortuous shoreline and complex tidal conditions, it is generally difficult to allocate sufficient number of tide gauge stations to control the precision of water level interpolation. In such cases the use of tide-surge models for determining waterline elevation would be a practical and effective method.

Acknowledgements

The authors would like to thank Dr. Xue Yunchuan for his suggestions on interpreting the remote sensing images for coastal areas. Thanks are also extended to the reviewers and the editor for their constructive comments and suggestions on the original manuscript.

References

Boak E H, Turner I L. 2005. Shoreline definition and detection: a review. Journal of Coastal Research, 21: 688–703

Chang Jun, Liu Gaohuan, Liu Qingsheng. 2004. Dynamic monitoring of coastline in the Yellow River Delta by remote sensing. Geo-Information Science (in Chinese), 6: 94–98

Chen L C, Rau J Y. 1998. Detection of shoreline changes for tideland areas using multi-temporal satellite images. Int J Remote Sensing, 19: 3383–3397

Dang Anrong, Jia Haifeng, Yi Shanzhen, et al. 2003. ArcGIS 8 Desktop application guide of Geographic Information System (in Chinese). 1st ed. Beijing: Tsinghua University Press, 289–293

Dang Anrong, Wang Xiaodong, Chen Xiaofeng, et al. 2003. ERDAS IMAGINE Remote Sensing Image Processing Method (in Chinese). 1st ed. Beijing: Tsinghua University Press, 187–192

Fang Guohong, Zheng Wenzhen, Wang Ji, et al. 1986. Tidal and Tidal Current Analysis and Prediction (in Chinese). Beijing: China Ocean Press

Frihy O E, Nasr S M, Hatta M M, et al. 1994. Remote sensing of beach erosion along the Rosetta promontary, northwestern Nile delta, Egypt. Int J Remote Sensing, 15: 1649–1660

Han Zhen, Yun Caixing, Jiang Xuezhong, et al. 2003. Deposition and erosion remote sensing inversion of tidal flat in Wenzhou area. Geography and Geo-Information Science (in Chinese), 19(6): 31–34

Huang Haijun, Li Chengzhi. 1998. A study on the present evolution of submarine radial sand ridges in the southern Yellow Sea using remote sensing images. Oceanologia et Limologia Sinica (in Chinese), 29: 640–645

Huang Haijun, Li Chengzhi, Guo Jianjun. 1994. Application of LANDSAT Images to the studies of the shoreline changes of the Huanghe River Delta. Marine Geology & Quaternary Geology (in Chinese), 14(2): 29–37

Jensen J R. 2007. Introductory Digital Image Processing: A Remote Sensing Perspective. 3rd ed. Beijing: China Science Press, 474–483

Kevin W, Hesham M. 1999. Monitoring changing position of coastlines using thematic mapper imagery: an example from the Nile Delta. Geomorphology, 29: 93–105

Lee K S, Kim T H, Yun Y S, et al. 2001. Spectral characteristics of shallow turbid water near the shoreline on intertidal flat. Korean Journal of Remote Sensing, 17(2): 131–139

Lee Y C, Qin Y S, Liu R Y. 1998. Yellow Sea Atlas. Seoul: Ho Yong Publishing Co, 100

Li Anlong, Li Guangxue, Cao Lihua, et al. 2004. The coastal erosion and evolution of the Yellow River Delta abandoned lob. Journal of Geographical Sciences (in Chinese), 59(5): 731–737

Lin Minji. 1991. Application of Remote Sensing to Ocean and Coastal Zone (in Chinese). Beijing: China Ocean Press, 184–193

Lin Hui, Lv Guonian, Song Zhiyao. 2000. Simulation and Research on Tidal Waves and Coast Evolution in the Bohai Sea, the Yellow Sea and the East China Sea (in Chinese). Beijing: China Science Press, 60–63

Mason D C, Amin M, Davenport I J, et al. 1999. Measurement of recent intertidal sediment transport in Morecambe Bay using the waterline method. Estuarine, Coastal and Shelf Science, 49: 427–456

Mason D C, Davenport I J, Flather R A, et al. 2001. A sensitivity analysis of the waterline method of constructing a digital elevation model for intertidal areas in ERS SAR scene of eastern England. Estuarine, Coastal and Shelf Science, 53: 759–778

Mason D C, Davenport I J, Robinson G J, et al. 1995. Construction of an intertidal digital elevation model by the 'water-line' method. Geophysical Research Letters, 22: 3187–3190

National Marine Data and Information Service (NMDIS). 2001. Tidal table 2002, v 1: from Estuary of Yalu River to Estuary of Yangtze River (in Chinese). Beijing: China Ocean Press

Ren Mei'e. 1986. Integrate Investigation Report of the Coastal Zone and Sea Resource in Jiangsu Province (in Chinese). Beijing: China Ocean Press

Ryu J H, Kim C H, Lee Y K, et al. 2008. Detecting the intertidal morphologic change using satellite data. Estuarine. Coastal and Shelf Science, 78: 623–632

Ryu J H, Won J S, Min K D. 2002. Waterline extraction from Landsat TM data in a tidal flat: a case study in Gomso Bay, Korea. Remote Sensing of Environment, 83: 442–456

Wang Ying. 2002. Radiative sandy ridge field on continental shelf of the Yellow Sea (in Chinese). Beijing: China Environment Science Press

Xu Hanxing. 1996. Tide Calculation (in Chinese). Beijing: China Communications Press

Yun Caixing. 2005. Application of Remote Sensing Techniques to Coastal Zone and Offshore Area (in Chinese). Beijing: China Ocean Press, 24–28

Zhang Zhende, Xiao Jichun. 1995. The application of remote sensing to investigate tidal flat evolution. Remote Sensing for Land & Resources (in Chinese), 3: 25–28

Zhao Yingshi. 2003. Remote Sensing Application Analysis Theory and Arithmetic (in Chinese). Beijing: China Science Press

Zhao Bin, Guo Haiqiang, Yan Yaner, et al. 2008. A simple waterline approach for tidelands using multitemporal satellite images: a case study in the Yangtze Delta. Estuarine, Coastal and Shelf Science, 77: 134–142

Zheng Zongsheng, Zhou Yunxuan, Jiang Xuezhong, et al. 2007. Waterline extraction and DEM reconstruction in Chongming Dongtan. Remote Sensing Technology and Application (in Chinese), 22: 35–38

Zhu Dakui, Fu Mingzhuo. 1986. Geomorphology and surficial sedimentary features of Dongsha sandbank. In: Ren Mei'e, Zhu Jiwen, Zhu Dakui, eds. Investigation Report of the Firstly Complete Survey on Dongsha sandbank (in Chinese). Beijing: China Ocean Press, 15–17